

Pyrazole-based allylpalladium complexes: Supramolecular architecture and liquid crystal behaviour

M.C. Torralba^a, M. Cano^{a,*}, J.A. Campo^a, J.V. Heras^a, E. Pinilla^{a,b}, M.R. Torres^b

^a Departamento de Química Inorgánica I, Facultad de Ciencias Químicas, Universidad Complutense, E-28040 Madrid, Spain

^b Laboratorio de Difracción de Rayos-X, Facultad de Ciencias Químicas, Universidad Complutense, E-28040 Madrid, Spain

Received 29 May 2006; accepted 22 July 2006

Available online 18 August 2006

Abstract

The co-ordination of non-mesomorphic 3-substituted pyrazoles Hpz^{R} to the $[\text{Pd}(\eta^3\text{-C}_3\text{H}_5)]^+$ fragment gives rise to four-coordinated complexes $[\text{Pd}(\eta^3\text{-C}_3\text{H}_5)(\text{Hpz}^{\text{R}})_2]^+$ ($\text{R} = \text{C}_6\text{H}_4\text{OC}_n\text{H}_{2n+1}$; $n = 12$ (**I**₁₂), 14 (**I**₁₄), 16 (**I**₁₆), 18 (**I**₁₈)), which were isolated with BF_4^- as counteranion. The new complexes are proved to have liquid crystal properties exhibiting monotropic or enantiotropic smectic A (SmA) mesophases at low temperatures which range between ca. 40 and 80 °C. The crystal structure of **I**₁₂ presents a 2D network highly interdigitated, which could be related with the layered structure proposed in the liquid crystalline phase through the X-ray diffraction at variable temperature.

© 2006 Elsevier B.V. All rights reserved.

Keywords: Palladium(II) complexes; Pyrazole; Metallomesogen; X-ray structure

For several years, we have been interested in the liquid crystal chemistry of substituted pyrazoles and the related pyrazolylpyridine ligands, as well as their metal complexes. In this context, we have proved that, in contrast to the mesomorphic nature of 3,5-bis(4-alkyloxyphenyl)pyrazole ($\text{Hpz}^{\text{R}2}$; $\text{R} = \text{C}_6\text{H}_4\text{OC}_n\text{H}_{2n+1}$) or 2-[3,5-bis(4-alkyloxyphenyl)pyrazol-1-yl]pyridine ($\text{pz}^{\text{R}2}\text{py}$) ligands [1–3], the 3-substituted homologues Hpz^{R} and $\text{pz}^{\text{R}}\text{py}$ did not exhibit liquid crystal behaviour [4–6]. However, it was interesting to note that all of them were able to induce mesomorphism upon co-ordination to determined palladium(II) fragments [2,3,5–7]. In particular, we have observed that the co-ordination of the mesogenic $\text{pz}^{\text{R}2}\text{py}$ ligands to PdCl_2 or $[\text{Pd}(\eta^3\text{-C}_3\text{H}_5)]^+$ fragments gave rise to metallomesogens [3,7] (Scheme 1). By contrast, the four-coordinated *cis*-dichloropalladium complexes $[\text{PdCl}_2(\text{pz}^{\text{R}}\text{py})]$ containing the related 3-substituted $\text{pz}^{\text{R}}\text{py}$ ligands were not mesomorphic, while their co-ordination to the $[\text{Pd}(\eta^3\text{-C}_3\text{H}_5)]^+$ moi-

ety yielded metallomesogenic derivatives [6] (Scheme 1), this feature suggesting the role of the electron delocalisation in the mesomorphism.

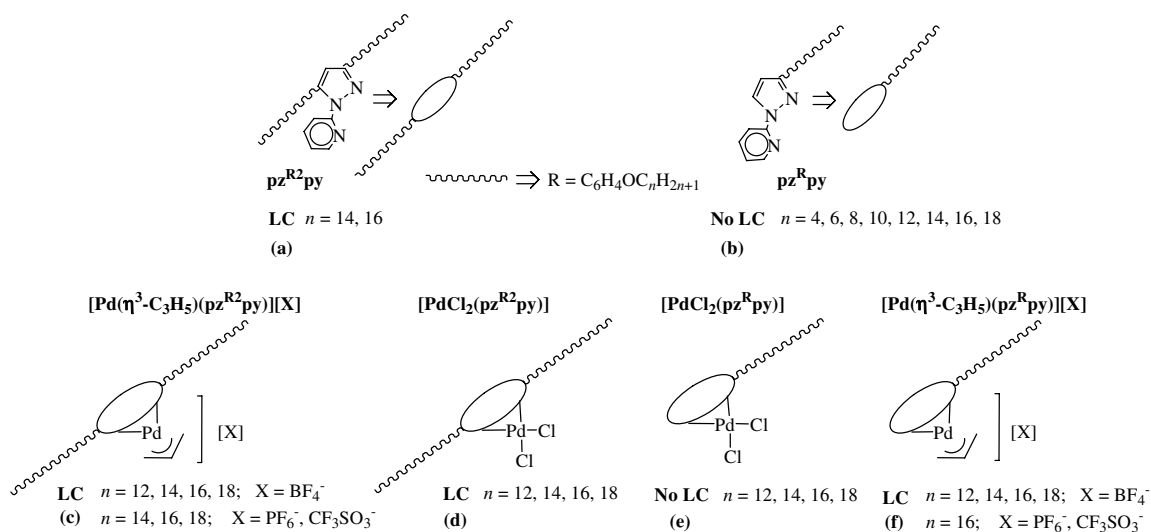
Following these results we decided to prove that the $[\text{Pd}(\eta^3\text{-C}_3\text{H}_5)]^+$ group can be useful as a candidate to produce metallomesogenic four-co-ordinated compounds by co-ordination to 3-(4-alkyloxyphenyl)pyrazole Hpz^{R} ligands (Scheme 2). We have already determined the mesomorphic properties of the related compounds *t*- $[\text{PdCl}_2(\text{Hpz}^{\text{R}})_2]$ [5].

In this work we describe the synthesis, characterisation and mesomorphic properties of a series of cationic compounds of the type $[\text{Pd}(\eta^3\text{-C}_3\text{H}_5)(\text{Hpz}^{\text{R}})_2]^+$ ($\text{R} = \text{C}_6\text{H}_4\text{OC}_n\text{H}_{2n+1}$; $n = 12$ (**I**₁₂), 14 (**I**₁₄), 16 (**I**₁₆), 18 (**I**₁₈)), which were isolated with BF_4^- as counteranion.

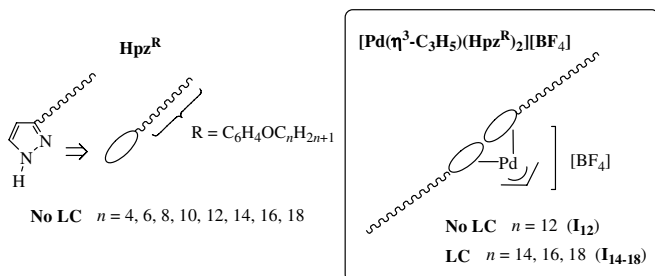
The syntheses of $[\text{Pd}(\eta^3\text{-C}_3\text{H}_5)(\text{Hpz}^{\text{R}})_2][\text{BF}_4]$ ($\text{R} = \text{C}_6\text{H}_4\text{OC}_n\text{H}_{2n+1}$; $n = 12$ (**I**₁₂), 14 (**I**₁₄), 16 (**I**₁₆), 18 (**I**₁₈)) [8] were carried out as it has been described for related compounds [6,7]. The spectroscopic (IR and ¹H NMR) and analytical data [9,10] allowed us to establish their identity and they are in agreement with the proposed formulation.

* Corresponding author. Fax: +34 91 3944352.

E-mail address: mmcano@quim.ucm.es (M. Cano).



Scheme 1. Schematic molecular representation and mesomorphic properties of the $\text{pz}^{\text{R}2}\text{py}$ (a) and $\text{pz}^{\text{R}}\text{py}$ (b) ligands, and their complexes $[\text{Pd}(\eta^3\text{-C}_3\text{H}_5)(\text{pz}^{\text{R}2}\text{py})][\text{X}]$ (c), $[\text{PdCl}_2(\text{pz}^{\text{R}2}\text{py})]$ (d), $[\text{Pd}(\eta^3\text{-C}_3\text{H}_5)(\text{pz}^{\text{R}}\text{py})][\text{X}]$ (e) and $[\text{PdCl}_2(\text{pz}^{\text{R}}\text{py})]$ (f) [3,6,7].



Scheme 2. Schematic molecular representation of the complexes $[\text{Pd}(\eta^3\text{-C}_3\text{H}_5)(\text{Hpz}^{\text{R}})_2][\text{BF}_4]$ (I_{12-18}) studied in this work.

The ^1H NMR spectra of I_{12-18} at room temperature in CDCl_3 solution show the expected resonances as broad signals attributed to a dynamic behaviour, which was proved by the analysis of their spectra at variable temperatures (from 30 to -50°C) [10]. This behaviour can be explained on the basis of the existence of different isomers related with the relative orientation of the allyl group and the two pyrazoles, which can interchange through a rotation of the allyl group or a tautomeric equilibrium. Many examples in the literature support this proposal [11].

The knowledge of the molecular structure of the mesophases has been a focus of interest in order to understand the liquid crystal behaviour of the compounds. In this context, we think that the X-ray structure of the studied complexes will contribute as a support for the establishment of potential structure/properties relationships. On this basis, we have solved the X-ray single-crystal structure of $[\text{Pd}(\eta^3\text{-C}_3\text{H}_5)(\text{Hpz}^{\text{ddp}})_2][\text{BF}_4]$ ($\text{Hpz}^{\text{ddp}} = 3\text{-(4-dodecyloxyphenyl)pyrazole}$) (I_{12}) (Fig. 1), as a representative member of the homologues studied in this work [12]. The crystal structure reveals that the complex is comprised of the BF_4^- anion and the cation $[\text{Pd}(\eta^3\text{-C}_3\text{H}_5)(\text{Hpz}^{\text{ddp}})_2]^+$, bonded through a strong H-bond (Table 1).

The four-co-ordination around the metal is defined by two nitrogen atoms from two *cis*-pyrazole groups and the two allyl C9 and C11 carbon atoms, in an almost square-planar geometry. It is deduced by the dihedral angle of $4.7(4)^\circ$ between the planes defined by the Pd, N1 and N3 atoms, and the Pd, C9 and C11 atoms. The Pd atom deviates $0.044(1)\text{ \AA}$ of the co-ordination plane defined by the N1, N3, C9 and C11 atoms. The Pd–N distances of ca. 2.08 \AA are similar to those found in related complexes [2,5,6,13–17]. The allyl group shows Pd–C distances of

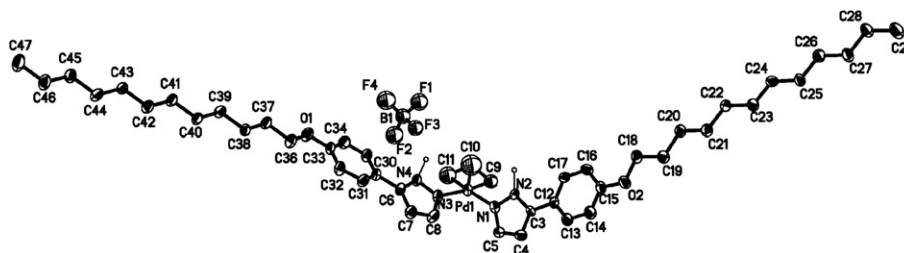


Fig. 1. Perspective ORTEP plot of $[\text{Pd}(\eta^3\text{-C}_3\text{H}_5)(\text{Hpz}^{\text{ddp}})_2][\text{BF}_4]$ (I_{12}). Hydrogen atoms, except H2 and H4, have been omitted for clarity. The thermal ellipsoids are at 30% probability level. Selected bond lengths (\AA) and angles ($^\circ$): Pd1–N1 2.085(8), Pd1–N3 2.079(8), Pd1–C9 2.10(1), Pd1–C10 2.10(2), Pd1–C11 2.09(1), C9–C10 1.381(5), C10–C11 1.374(5), N1–Pd1–N3 92.9(3), N1–Pd1–C9 99.1(4), N1–Pd1–C10 132.3(4), N1–Pd1–C11 166.6(5), N3–Pd1–C9 167.9(4), N3–Pd1–C10 131.1(4), N3–Pd1–C11 99.7(5), C9–Pd1–C10 38.4(2), C9–Pd1–C11 68.2(5), C10–Pd1–C11 38.3(2), C9–C10–C11 117(2).

Table 1
Hydrogen-bond geometries for **I**₁₂

D–H···A	<i>d</i> (D–H) (Å)	<i>d</i> (H···A) (Å)	<i>d</i> (D···A) (Å)	∠(D–H···A) (°)
N4–H4···F3	1.28	1.87	2.98(1)	141.3
N2–H2···F1 ^a	1.27	1.86	3.04(1)	151.8
C5–H5···F1 ^b	0.93	2.46	3.31(1)	150.5

^a 1 – *x*, –*y* + 1, –*z*.

^b *x*, –*y* + 3/2, –*z* + 1/2.

ca. 2.10 Å, in agreement with that observed in other Pd-compounds containing N-donor ligands [6,13–17].

The C9C10C11 allyl group is slightly deviated from the ideal geometry, with bond distances of ca. 1.38 Å and an C–C–C angle of 117(2)°. The central C10 carbon atom presents a deviation of 0.65(2) Å of the co-ordination plane.

The benzene planes of the substituents are slightly twisted with respect to their own pyrazole planes with dihedral angles of 15.6(4) and 14.2(4)°. The two alkyl chains point in an almost opposite direction with an angle of 63.9(1)° which is defined as that formed between the lines O2–C29 and O1–C47.

On the other hand, it has been established that in related [Pd(η³-C₃H₅)(Hpz)₂]⁺ derivatives, the two *cis*-pyrazole can adopt different orientations of the NH-groups which can be determinant for the supramolecular architecture [16,17]. In the current compound, the pyrazole planes form an dihedral angle of 71.9(3)°, and the torsion angle τ defined by the four N-atoms of the two pyrazoles involved in the

whole cation is 26(2)°. As a consequence, the two NH-groups interact with two different BF₄[–] counteranions through strong H-bonds (Table 1). Each BF₄[–] group bridges two cationic entities, as it had been observed in related compounds exhibiting polymeric chains and an torsion angle τ of ca. 180° [16–18]. However, at difference to those, in our compound, two BF₄[–] counteranions bond the same two cationic unities so generating dimers through these N–H···F interactions (Fig. 2).

New weak C–H···F interactions between the dimers (Table 1) give rise to layers defining a 2D structure that is highly interdigitated (Fig. 3).

The thermal behaviour of the new complexes **I**_{12–18} was studied by differential scanning calorimetry (DSC), polarised light optical microscopy (POM) and X-ray diffraction at variable temperature (XRD). The phase transition temperatures and thermodynamic data are given in Fig. 4. Complex **I**₁₂ was non-mesomorphic showing only a melting process at 73 °C. The remaining compounds **I**_{14–18} displayed monotropic (**I**₁₄ and **I**₁₆) or enantiotropic (**I**₁₈) liquid crystal properties exhibiting smectic A (SmA) mesophases (Fig. 5), which were identified from the battonets and homeotropic textures observed by POM.

For compounds **I**₁₄ and **I**₁₆, the transition from the mesophase to crystal could not be determined since the crystalline phase appears at lower temperatures than 40 °C. Then, on reheating from 40 °C, a simple clearing event at 60 and 71 °C, respectively, is observed by POM and DSC. The third heat–cool cycle reproduces the second exactly.

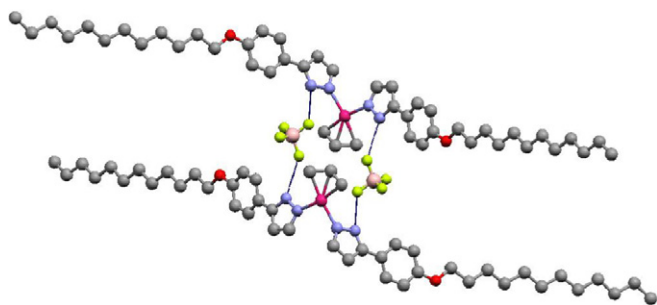


Fig. 2. Dimeric unit of **I**₁₂ showing the N–H···F hydrogen bonds.

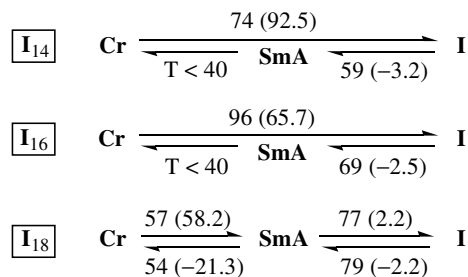


Fig. 4. Phase properties on the first heat–cool cycle of **I**_{14–18}. Onset temperatures (°C) and enthalpies (kJ mol^{–1}, in parentheses) are given.

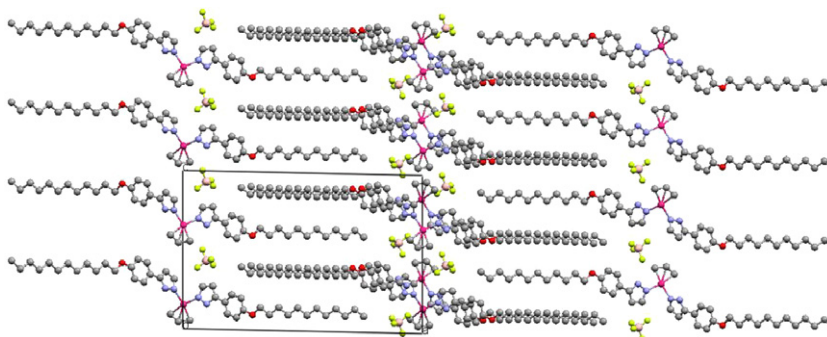


Fig. 3. 2D network of **I**₁₂ viewed in the *ac* plane.

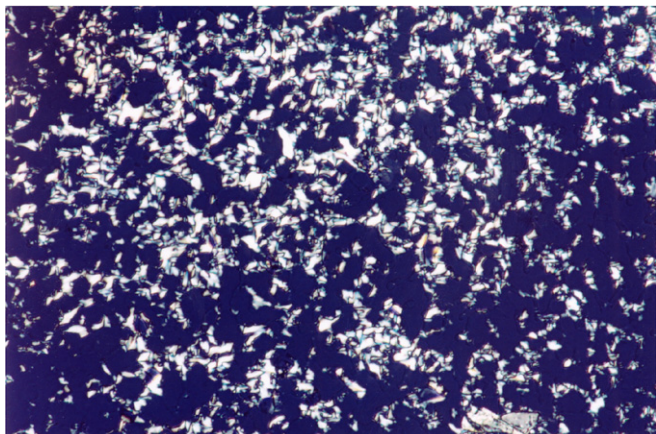


Fig. 5. Texture of the smectic A mesophase, observed on cooling, for I_{16} at 71 °C.

The enantiotropic behaviour of I_{18} was confirmed by the DSC trace observed in the first heating, which shows two phase transitions related with the melting Cr–SmA and clearing SmA–I processes (Fig. 4). Successive heat–cool cycles reproduce the same behaviour. The enantiotropic SmA phase in I_{18} can be related to a larger molecular isotropy produced by the presence of longer chains.

As a representative example, X-ray diffraction experiments at variable temperature were undertaken for I_{14} in order to examine the mesomorphic structure of these compounds. At 50 °C on cooling, the diffractogram exhibits two small-angle peaks at 40.9 and 21.0 Å, and a broad halo at ca. 4.5 Å corresponding to the fluid behaviour of the alkyl chains. The former ones from the (001) and (002) reflections agree with a lamellar structure from the SmA phases observed by POM. At 25 °C, on cooling, the pattern observed corresponds neither to a crystalline phase nor to a liquid crystal phase. This result could be attributed to the presence of a smectic glassy phase in accordance with the no evidence of crystallisation established from the POM observations.

The length of the cationic part in the most extended crystalline conformation, calculated on the basis of the X-ray structure of I_{12} commented above, was estimated to be of ca. 52 Å, and the value of the spacing was 40.9 Å. Therefore these results reveal some interdigitation of the layers, as it has been observed in the packing of I_{12} (Fig. 3).

Supplementary material

Crystallographic data of I_{12} have been deposited with the Cambridge Crystallographic Data Centre (CCDC deposition number 609242).

Acknowledgements

Financial support from the DGI of the Ministerio de Educación y Ciencia (Project No. BQU2003-07343) and

Universidad Complutense (UCM2005-910300) is gratefully acknowledged. We also thank Comunidad de Madrid for financial support (Project GR/MAT/0511/2004) and the contract to M.C.T.

References

- [1] M.C. Torralba, M. Cano, J.A. Campo, J.V. Heras, E. Pinilla, M.R. Torres, *J. Organomet. Chem.* 654 (2002) 150.
- [2] M.C. Torralba, M. Cano, S. Gómez, J.A. Campo, J.V. Heras, J. Perles, C. Ruiz-Valero, *J. Organomet. Chem.* 682 (2003) 26.
- [3] M.J. Mayoral, M.C. Torralba, M. Cano, J.A. Campo, J.V. Heras, *Inorg. Chem. Commun.* 6 (2003) 626.
- [4] M.C. Torralba, M. Cano, J.A. Campo, J.V. Heras, E. Pinilla, M.R. Torres, *J. Organomet. Chem.* 633 (2001) 91.
- [5] M.C. Torralba, M. Cano, J.A. Campo, J.V. Heras, E. Pinilla, M.R. Torres, *Inorg. Chem. Commun.* 5 (2002) 887.
- [6] M.C. Torralba, M. Cano, J.A. Campo, J.V. Heras, E. Pinilla, M.R. Torres, *J. Organomet. Chem.* 691 (2006) 765.
- [7] M.C. Torralba, J.A. Campo, J.V. Heras, D.W. Bruce, M. Cano, *Dalton Trans.* (2006) 3918.
- [8] To a colourless acetone solution (20 mL) of $[\text{Pd}(\eta^3\text{-C}_3\text{H}_5)(\text{acetone})_2][\text{BF}_4]$, prepared from $[\text{Pd}(\mu\text{-Cl})(\eta^3\text{-C}_3\text{H}_5)]_2$ (100 mg, 0.273 mmol) and AgBF_4 (106.3 mg, 0.546 mmol) according to described procedures [6,7], was added the stoichiometric amount (0.546 mmol) of the corresponding pyrazole Hpz^R ligand [4,5] in acetone (40 mL). After 24 h of stirring under nitrogen at room temperature, the solvent was removed *in vacuo* and the solid crystallised from dichloromethane/hexane leading to the precipitation of a colourless solid, which was filtered off, washed with hexane and dried *in vacuo*.
- [9] I_{12} : Yield: 79%. Elemental analyses: found C 60.2, H 7.5, N 6.3%; calculated for $\text{C}_{45}\text{H}_{69}\text{BF}_4\text{N}_4\text{O}_2\text{Pd}$: C 60.6, H 7.5, N 6.3%. IR(KBr, cm^{-1}): 3330 $\nu(\text{NH})$, 1616 $\nu(\text{CN})$, 1096–1006 $\nu(\text{BF})$, 519 $\delta(\text{FBF})$. I_{14} : Yield: 80%. Elemental analyses: found C 60.3, H 7.8, N 5.7%; calculated for $\text{C}_{49}\text{H}_{77}\text{BF}_4\text{N}_4\text{O}_2\text{Pd} \cdot 1/2\text{CH}_2\text{Cl}_2$: C 60.1, H 7.9, N 5.7%. IR(KBr, cm^{-1}): 3323 $\nu(\text{NH})$, 1617 $\nu(\text{CN})$, 1099–1020 $\nu(\text{BF})$, 521 $\delta(\text{FBF})$. I_{16} : Yield: 50%. Elemental analyses: found C 62.5, H 8.1, N 5.3%; calculated for $\text{C}_{53}\text{H}_{85}\text{BF}_4\text{N}_4\text{O}_2\text{Pd} \cdot 1/3\text{CH}_2\text{Cl}_2$: C 62.2, H 8.4, N 5.4%. IR(KBr, cm^{-1}): 3326 $\nu(\text{NH})$, 1615 $\nu(\text{CN})$, 1099–1016 $\nu(\text{BF})$, 521 $\delta(\text{FBF})$. I_{18} : Yield: 84%. Elemental analyses: found C 64.3, H 8.4, N 5.6%; calculated for $\text{C}_{57}\text{H}_{93}\text{BF}_4\text{N}_4\text{O}_2\text{Pd}$: C 64.6, H 8.8, N 5.3%. IR(KBr, cm^{-1}): 3331 $\nu(\text{NH})$, 1615 $\nu(\text{CN})$, 1094–1035 $\nu(\text{BF})$, 525 $\delta(\text{FBF})$.
- [10] ^1H NMR data of I_{12} (CDCl_3 , 248 K; δ , ppm; J , Hz): Major signals: 12.00, 11.90, 11.82 (NH); 7.91 ($^3J=8.7$), 7.56 ($^3J=8.7$), 7.54 ($^3J=8.6$) (*Ho* of C_6H_4); 7.67, 7.42, 6.78 (*H5* of pyrazole); 7.02 ($^3J=8.7$), 6.94 ($^3J=8.6$) (*Hm* of C_6H_4); 6.54, 6.51, 6.34 (*H4* of pyrazole); 5.80 (*Hmeso* of allyl); 4.07 ($^3J=6.6$), 4.03 ($^3J=6.4$), 4.01 ($^3J=6.6$) (*Hsyn* of allyl); 3.35 ($^3J=12.2$), 3.32 ($^3J=12.4$), 3.22 ($^3J=12.5$) (*Hanti* of allyl); 3.95 (OCH_2); 1.8–1.1 (CH_2); 0.85 ($^3J=6.6$) (CH_3). Minor signals: 11.70 (NH); 7.33 ($^3J=8.4$) (*Ho* of C_6H_4); 6.77 ($^3J=8.4$) (*Hm* of C_6H_4); 6.43 (*H4* of pyrazole); 3.86 ($^3J=6.8$) (*Hsyn* of allyl); 3.05 ($^3J=12.3$) (*Hanti* of allyl); the remaining resonances are masked by the major signals.
- [11] F.A. Jalón, B.R. Manzano, B. Moreno-Lara, *Eur. J. Inorg. Chem.* (2005) 100, and References therein.
- [12] Colourless prismatic single-crystals ($0.60 \times 0.07 \times 0.06 \text{ mm}^3$) were obtained from dichloromethane/hexane solution. *Crystal data*: $\text{C}_{45}\text{H}_{69}\text{BF}_4\text{N}_4\text{O}_2\text{Pd}$; M_r 891.25; T 293(2) K; λ 0.71073 Å; *Bruker-Smart CCD* diffractometer (operating at 50 kV and 30 mA); monoclinic, space group $P2_1/c$, $a = 27.562(2)$ Å, $b = 9.3437(8)$ Å, $c = 18.190(2)$ Å, $\beta = 91.203(2)^\circ$, $V = 4683.5(7)$ Å³, $Z = 4$, $D_c = 1.264 \text{ g cm}^{-3}$, $\mu = 0.451 \text{ mm}^{-1}$. The data were collected over a hemisphere of the reciprocal space by combination of three exposure sets. The cell parameters were determined and refined by least-squares fit of all reflections collected [θ range = 1.48–25.00°; index

range = (−32, −11, −18) to (29, 11, 21)]. Each exposure of 20 s covered 0.3° in ω . The first 50 frames were recollected at the end of the data collection to monitor crystal decay. No appreciable decay in the intensities of standard reflections was observed. The structure was solved by direct methods and refined by full-matrix least-squares on F^2 [19]. All non-hydrogen atoms were refined anisotropically with the exception of the BF_4 and allyl groups, which have been refined isotropically and in the last cycles, the thermal parameters were fixed. The carbon atoms of the allyl group were refined with geometrical restraints and a variable common carbon–carbon distance. All hydrogen atoms were included in calculated positions, except H2 and H4 bonded to N2 and N4, respectively, which were located in a *Fourier* synthesis. All hydrogen atoms were refined as riding on their respective bonded atoms. The final R indices with $I > 2\sigma(I)$ was 0.072 for 2620 observed reflections, while wR_2 for all data (8231 independent reflections, $R_{\text{int}} = 0.1416$) was 0.231. The GOF (F^2) was 0.855, and the largest residual peak and hole in the final difference map were 1.018 and $-0.834\text{e}\text{\AA}^{-3}$, respectively.

- [13] M.C. Torralba, M. Cano, J.A. Campo, J.V. Heras, E. Pinilla, M.R. Torres, J. Perles, C. Ruiz-Valero, *J. Organomet. Chem.* 691 (2006) 2614.
- [14] F. Gómez-de la Torre, A. de la Hoz, F.A. Jalón, B.R. Manzano, A. Otero, A.M. Rodríguez, M.C. Rodríguez-Pérez, *Inorg. Chem.* 37 (1998) 6606.
- [15] F. Gómez-de la Torre, A. de la Hoz, F.A. Jalón, B.R. Manzano, A.M. Rodríguez, J. Elguero, M. Martínez-Ripoll, *Inorg. Chem.* 39 (2000) 1152.
- [16] M. Cano, J.V. Heras, M.L. Gallego, J. Perles, C. Ruiz-Valero, E. Pinilla, M.R. Torres, *Helv. Chim. Acta* 86 (2003) 3194.
- [17] R.M. Claramunt, P. Cornago, M. Cano, J.V. Heras, M.L. Gallego, E. Pinilla, M.R. Torres, *Eur. J. Inorg. Chem.* (2003) 2693.
- [18] M.L. Gallego, M. Cano, J.A. Campo, J.V. Heras, E. Pinilla, M.R. Torres, *Helv. Chim. Acta* 88 (2005) 2433.
- [19] G.M. Sheldrick, 'SHELXL97, Program for Refinement of Crystal Structure', University of Göttingen, Göttingen, Germany, 1997.